Engineered Science
DOI: https://dx.doi.org/10.30919/es961

Multi-Objective Optimization of Process Parameters in Milling of 17-4 PH Stainless Steel using Taguchi-based Gray Relational Analysis

Fuat Kara,[1,*] Nurettin Bulan,[2] Mahir Akgün[3] and Uğur Köklü[4]

Abstract

The present study investigates the effects of cutting parameters and the variation of nose radius on cutting force, surface roughness, cutting temperature, and tool wear in the milling 17-4 PH stainless steel. The milling experiments were carried out using the Taguchi L18 experimental design with two different types of cutting nose radius (0.4 and 0.8), three different cutting speeds (70, 140 and 210 m/min), three different feed rates (0.06, 0.09 and 0.12 mm/tooth), and a constant cutting depth (1 mm). The outcomes of this study show that the cutting force, cutting temperature, and tool wear values are average 2.35, 28.89 and 1.18% lower when 17-4 PH stainless steel is machined with a 0.4 mm cutting nose radius compared to those in a 0.8 mm cutting nose radius. The surface quality is also improved by average 47.48% with an increase in the cutting tool nose radius. According to the multi response optimization results, the optimal levels of milling parameters for multiple output parameters are determined as 0.8 mm cutting nose radius, 70 m/min cutting speed and 0.06 mm/tooth, respectively.

Keywords: 17-4 PH stainless steel, Machining; Milling, Grey relational analysis; Optimization.
Received: 07 August 2023; Revised: 25 August 2023; Accepted: 25 August 2023.
Article type: Research article.

1. Introduction

Stainless steels in the group of high alloy steels contain high rates of nickel and chromium. These steels have many superior properties such as higher strength, corrosion resistance, higher hardness, ductility, hardness, and heat resistance due to the presence of these alloying elements in their chemical components.[1,2] 17-4 PH steel, one of the stainless steels, is a highly preferred type of stainless steel in applications requiring high strength in recent years. This steel is martensitic stainless steel that contains significant amounts of copper as well as nickel and chromium in its structure and is hardenable by precipitation.[3] The tensile and fatigue strength of this steel increases with the homogeneous dispersion of the copper-rich precipitates in the martensite phase.[4] Due to these properties, it is used in various applications in aerospace, marine, energy, mining, and automobile.[5,6] Stainless steels are well known as difficult-to-machine materials because of their high ductility and low thermal conductivity in the machining industry.[7,8] During the machining of these steels, in addition to excessive wear on the cutting tool, chip accumulation (BUE) and continuous chip formation occur at the cutting edge, which affects machining characteristics.[9,10] Since hard and continuous chips are formed due to high alloying elements, it is recommended to prefer carbide cutting tools with chip breakers.[11] In the machining of these steels, on the other hand, it can be applied in different optimization techniques and empirical models to reach optimal machining conditions in the context of reducing tooling costs and increasing machining efficiency. When the studies on the machining of PH stainless steels, which are the subject of the study, are evaluated in the literature, Sivaiah and Chakradhar[12] studied the effect of cryogenic coolant on cutting temperature, tool wear, surface

[1] *Department of Mechanical Engineering, Duzce University, Duzce8 1620, Turkey.*
[2] *Graduate School of Natural and Applied Sciences, Düzce University, 81620, Düzce, Turkey.*
[3] *Department of Machine and Metal Technology, Technical Sciences Vocational School, Aksaray University, Aksaray 68100, Turkey.*
[4] *Department of Mechanical Engineering, Karamanoğlu Mehmetbey University, Karaman 70100, Turkey.*
**Email:* fuatkara@duzce.edu.tr (F. Kara)

integrity and chip morphology under different cooling conditions in turning of 17-4 PH stainless steel. The authors stated that the cutting temperature, flank wear and surface roughness decreased by 71%, 48% and 27%, respectively, in the cryogenic machining compared to dry machining. In another study, they applied the Taguchi based grey relational analysis to assess the machinability performance of 17-4 PH stainless steel under cryogenic cooling environment.[13] The authors reported that Taguchi based gray relational analysis decrease the time and material waste and so can be suggested for use in machining of 17-4 PH stainless steel. Khanna *et al*.[14] studied the effects of different cooling conditions on turning performance characteristics during machining of 15-5 PH stainless steel. The researchers found that hybrid nanoparticles immersed EMQL method is clearly better than dry machining in terms of energy consumption. Cetin and Kıvak[15] studied to optimize the processing parameters in the machining of 15-5 PH stainless steel with PVD TiAlN/AlCrO and CVD TiCN/Al_2O_3/TiN coated inserts. The authors stated that CVD TiCN/Al_2O_3/TiN coated insert is obviously better than PVD TiAlN/AlCrO insert in terms of surface roughness and cutting force. Ganta and Chakradhar applied the grey relational analysis to optimize cutting parameters in hot machining of 15-5 PH stainless steel. The authors observed that the performance characteristics (surface roughness and metal removal rate) are significantly influenced by the cutting speed. Vignesh *et al*.[16] studied the effects of machining parameters on cutting forces and tool wear in turning of 17-4 PH stainless steel using cryogenic treated and untreated WC insert. The authors stated that cutting forces were lower in cryogenically treated inserts compared to conventional inserts, and accordingly, less flank wear occurred. Ondin *et al*.[17] compared the turning performance of 13-8 PH stainless steel under MQL conditions. The authors observed that MWCNTs nanoparticles assisted MQL is generally a more efficient method than dry and MQL. Recently, the authors have been performed the experimental works on evaluating turning performance characteristics during machining of 17-4 PH stainless steel under different cooling conditions (cryogenic, wet, MQL and dry).[18,19] The researchers also applied optimization techniques to predict turning performance characteristics.[20-22] However, the studies about milling performance characteristics of 17-4 PH stainless steel are very limited.[23] The performance characteristic measured in turning operation cannot be directly applied to milling due to the intermittent nature of the milling operation.[24]

Based on the literature review, it can be seen that limited studies were conducted on the milling of 17-4 PH stainless steel. Moreover, there is no information on the influence of the tool corner radius on the cutting temperature, cutting force, surface roughness and tool wear during milling of 17-4 PH stainless steel. Therefore, the current study aimed to optimize the milling performance characteristics simultaneously and to investigate the effect of the corner radius on these performance characteristics.

2. Materials and methods

The workpiece material utilized in the experiments was 17-4 PH stainless steel having the dimensions of 150 × 100 × 50 mm. The milling tests were performed on a Quaser MV154C-18.5 kW CNC vertical machining center at four cutting speeds (70, 140, and 210 m/min), three feeds (0.06, 0.09, and 0.12 mm/tooth), and a depth of cut (1 mm) under dry cutting conditions. The milling tests used the PVD-TiAlN-TiN coated tools with 0.4 mm and 0.8 mm insert radius. These cutting tools were produced by TaeguTec company in TT8080 quality and with ISO geometry 3PKT 100404R-M and 3PKT 100408R-M. Fig. 1 shows the image and information of the cutting tool. Furthermore, these cutting tools were clamped mechanically on a rigid tool holder (its code was 3P TE90-116-W16-10).

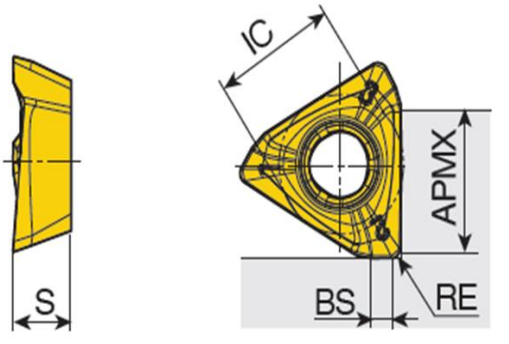

Designation	IC	RE	BS	S	APMX
3PKT 100404R-M	6.90	0.40	1.30	4.00	7.00
3PKT 100408R-M	6.90	0.80	0.90	4.00	7.00

Fig. 1 Cutting tool and information.

Kistler 9257B type dynamometer and equipment were used to measure the cutting force components occurring in the milling experiments. At the same time, the cutting temperature occurred in each experiment was measured by using OPTRIS brand PI 450 model thermal camera. Temperature measurements can be made to 900 °C with this thermal camera. The emissivity value was chosen as 0.8 to measure the cutting temperature value of the workpiece material. Furthermore, the roughness measurements have been performed using a Zygo ZeGage optical profilometer. To determine the surface roughness values, the workpiece was placed on the table of the

optical profilometer device in parallel after the milling process, and measurements were made from three different points. The surface roughness values were obtained by taking the average of these measurements. Finally, tool wear tests were carried out to evaluate the wear performance of the cutting tools under all cutting conditions. These experiments were carried out by determining the chip volume to be removed according to the cutting speeds and feed rates. After every 100 mm machining length, the cutting process was stopped, and the wear amount of the cutting tool was measured using the Insize brand digital microscope. The amount of wear in the cutting tools was evaluated depending on the chip volume. The schematic representation of the experimental setup is given in Fig. 2.

3. Experimental design and optimization

The Taguchi method is widely used in engineering analysis as it minimizes production costs and increases efficiency. In particular, this method is also known for significantly reducing the number of tests by using orthogonal arrays and minimizing the effects of uncontrollable factors. Therefore, the milling tests have been designed using Taguchi L_{18} orthogonal array. The cutting tool nose radius (r), cutting speed (Vc), and feed rate (f) has been selected as the input parameters. On the other hand, the main cutting force (Fc), cutting temperature (T), and surface roughness (Ra) and tool wear (Vb) has been selected as the output parameters. The S/N analysis was applied to calculate the S/N ratios of each level of process parameters. In calculating S/N signal-to-noise ratios to obtain the lowest output parameters values, the "smallest best" approach in Eq. (1) is preferred.[25] Then, variance analysis (ANOVA) was performed to determine the individual interactions of process factors.[26]

$$n = \frac{S}{N} = -10\log\left(\frac{1}{n}\sum_{i=1}^{n} y_i^2\right) \quad (1)$$

In addition to obtaining the most suitable conditions for a single output parameter, it has been also aimed to optimize all output parameters simultaneously for maximum efficiency. Therefore, the input parameters' optimum levels were found simultaneously by using GRA for the output parameters (Fc, T, Ra, and Vb). Taguchi-based GRA methodology steps applied in this study are given in Table 1.[27]

Table 1. Stages of the Taguchi-based GRA methodology.

Steps	Definitions and formulas
1	The reference sequence of length n is as follows; $x_0 = (x_0(1), x_0(2), x_0(3), \ldots, x_0(n))$
2	Data normalization; the smaller-the better $x_i(k) = \frac{\max x_i^0(k) - x_i^0(k)}{\max x_i^0(k) - \min x_i^0(k)}$
3	The gray relationship coefficient; $n\left(x_0(0), x_j(k)\right) = \frac{n_{min} + \zeta n_{max}}{n_{0i}(k) + \zeta n_{max}}$ ζε is a coefficient between (0.1). j=1, 2, … m; k= 1, 2, … n. the ζ function sets the difference between $n_{0i}(k)$ and n_{max}
4	Grey relational degree is calculated by equation; ıf impact on the performance of the output is equal; $\gamma(x_0, x_i) = \frac{1}{n}\sum_{n}^{k=1} n\left(x_0(k), x_j(k)\right)$ If impact on the performance of the output is not equal; $\gamma(x_0, x_i) = \frac{1}{n}\sum_{k=1}^{n} \varepsilon\left(x_0(k), x_j(k)\right)$ γ ranges from zero to one, 'n' is the number of performance measures.
5	Determination of the new levels of the input parameters
6	Implementation of taguchi method; calculation of s/n ratios and response table

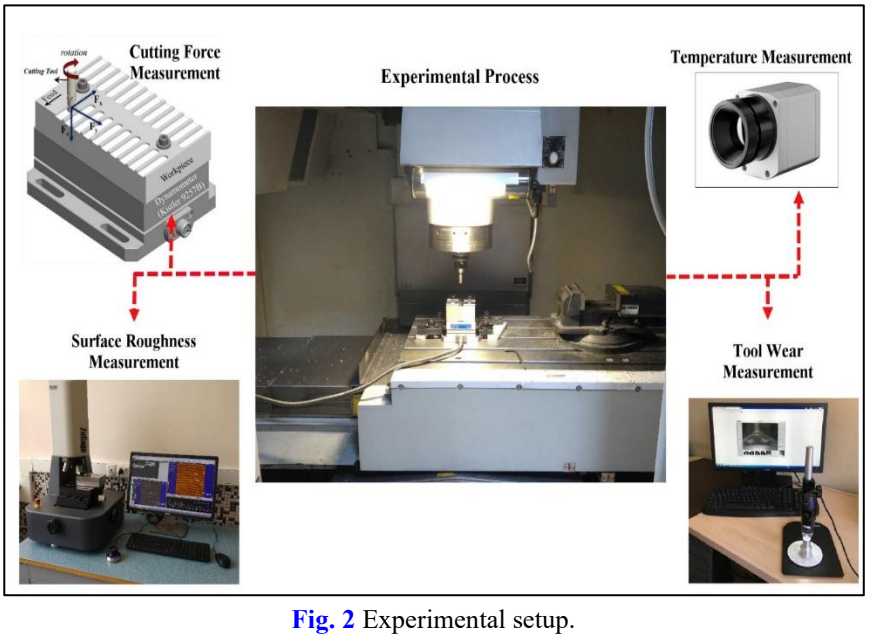

Fig. 2 Experimental setup.

Table 2. Experiment results.

Test Id	Parameters A (r)	B (Vc)	C (f)	Fc (N)	Ra (μm)	T (°C)	Vb (mm)
1	0.4	70	0.06	97.42	0.403	168	0.165
2	0.4	70	0.09	103.62	0.487	174	0.181
3	0.4	70	0.12	125.54	0.518	208	0.196
4	0.4	140	0.06	87.62	0.354	193	0.174
5	0.4	140	0.09	110.91	0.394	217	0.179
6	0.4	140	0.12	120.36	0.490	221.6	0.182
7	0.4	210	0.06	86.45	0.341	231.7	0.191
8	0.4	210	0.09	100.88	0.372	238	0.206
9	0.4	210	0.12	125.82	0.397	264	0.222
10	0.8	70	0.06	100.78	0.265	228	0.178
11	0.8	70	0.09	120.19	0.278	247	0.179
12	0.8	70	0.12	141.93	0.317	256.6	0.181
13	0.8	140	0.06	97.52	0.184	253	0.184
14	0.8	140	0.09	116.85	0.234	259.1	0.187
15	0.8	140	0.12	123.25	0.228	274.3	0.191
16	0.8	210	0.06	92.50	0.141	298.3	0.196
17	0.8	210	0.09	102.65	0.157	311	0.198
18	0.8	210	0.12	128.75	0.168	341	0.199

Table 3. S/N response of experiment results.

	Cutting factors					
	A (Ct)	B (Vc)	C (*f*)	A (Ct)	B (Vc)	C (*f*)
Fc				*Ra*		
1	-40.65	-40.96	-39.44	7.680	8.748	11.565
2	-40.80	-40.64	-40.62	13.474	10.578	10.458
3		-40.57	-42.11		12.405	9.708
Delta	0.15	0.39	2.66	5.794	3.656	1.857
T				*Vb*		
1	-46.48	-46.48	-47.04	14.53	14.90	14.84
2	-48.70	-47.41	-47.51	14.52	14.76	14.51
3		-48.88	-48.22		13.90	14.21
Delta	2.22	2.40	1.18	0.01	1.00	0.63

4. Results and discussion

4.1 Analysis of the signal-to-noise (S/N) ratio

Cutting force, surface roughness, cutting temperature, and tool wear were measured in the experiments designed using the Taguchi technique. The lowest values of cutting force, surface roughness, cutting temperature and tool wear are very important for productivity in machining. Therefore, the "lowest is best" equation was used to calculate the signal-to-noise (S/N) ratio in optimizing the measured output parameters.[28] The results of the experiments performed according to the Taguchi L18 index are given in Table 2. The S/N ration analysis results for the output parameters are given in Table 3 and shown graphically in Fig. 3. According to the S/N ratios, the optimal combination of process parameters for Fc, Ra, T and Vb is found to be: $A_1B_3C_1$, $A_2B_3C_1$ $A_1B_1C_1$ and $A_1B_1C_1$, respectively.

4.2 ANOVA

ANOVA has been applied to determine the individual interactions of control factors on output parameters.[29,30] The ANOVA results for the output parameters are shown in Table 4. From Table 4, considering the contribution rates of the control factors for each output parameter, it was found that the feed rate (85.50%), cutting nose radius (73.91%), cutting nose radius (48.70), and cutting speed (57.27%) were the most effective control factors on the cutting force, surface roughness, cutting temperature, and tool wear, respectively.

4.3 Cutting force

The variation in the main cutting force against different cutting parameters has been presented in Fig. 4. According to Fig. 4(a), (b) and (c), the lowest cutting force (86.45 N) was obtained at 210 m/min cutting speed, 0.06 mm/tooth feed rate and 0.4 mm cutting nose radius, while the highest cutting force (141.93 N) was obtained at 70 m/min cutting speed, 0.12 mm/tooth feed rate and 0.8 mm cutting nose radius. In other words, according to the average force value measured when milling 17-4 PH stainless steel with 0.4 mm cutting nose radius, a 2.35% increase was observed in the measured mean force value when milling 17-4 PH stainless steel with 0.8 mm cutting nose radius. There are many reasons for this; first, with the increase

of cutting nose radius, the specific cutting energy increases, resulting in greater cutting forces.[31] Another reason is that the shear angle responsible for the large shear plane in the primary deformation zone, decreases and the chip thickness increases.[32] The increasing trend in cutting force is also seen in feed rate and it can be clearly seen in Fig. 4 that the feed rate plays a more effective role compared to other cutting parameters. As can be seen from Fig. 4, for 0.4- and 0.8-mm cutting nose radius, the Fc values have about a 6 and 12% increase with a 50% increase of feed rate while this increased

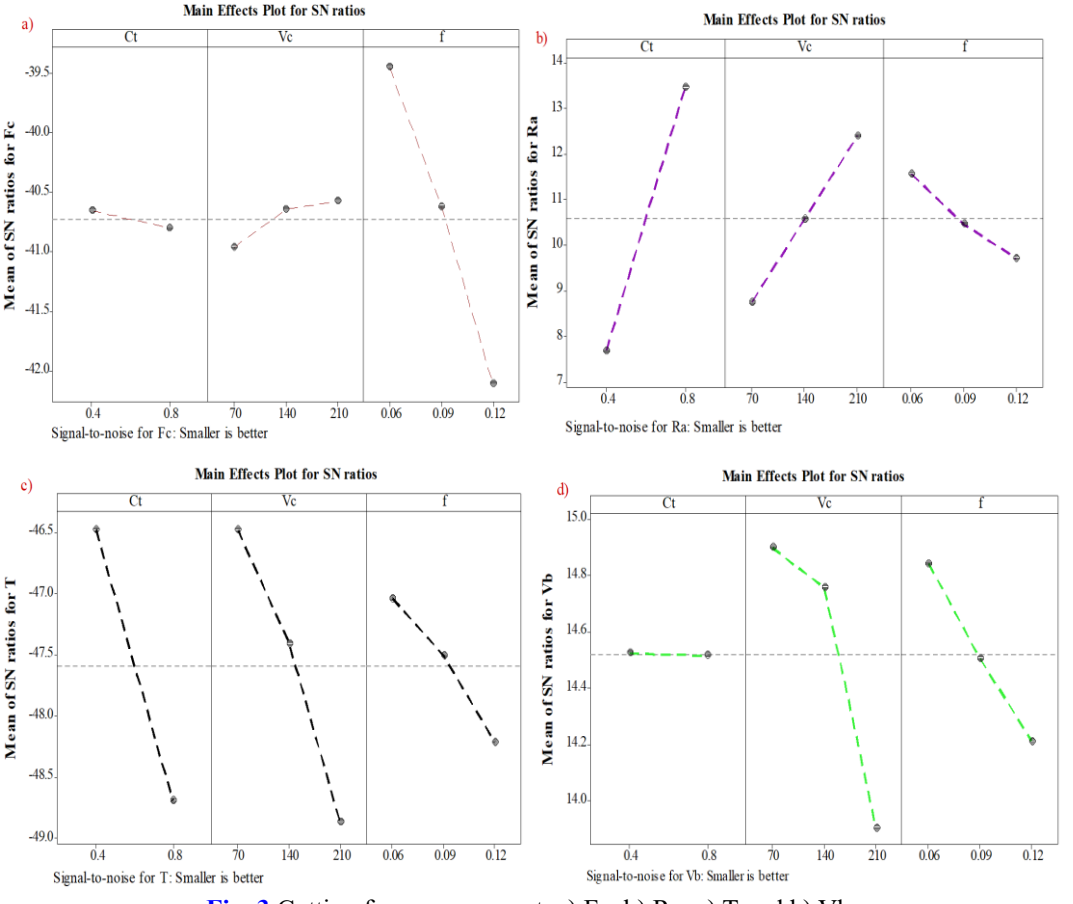

Fig. 3 Cutting force assessment, a) Fc, b) Ra, c) T and b) Vb.

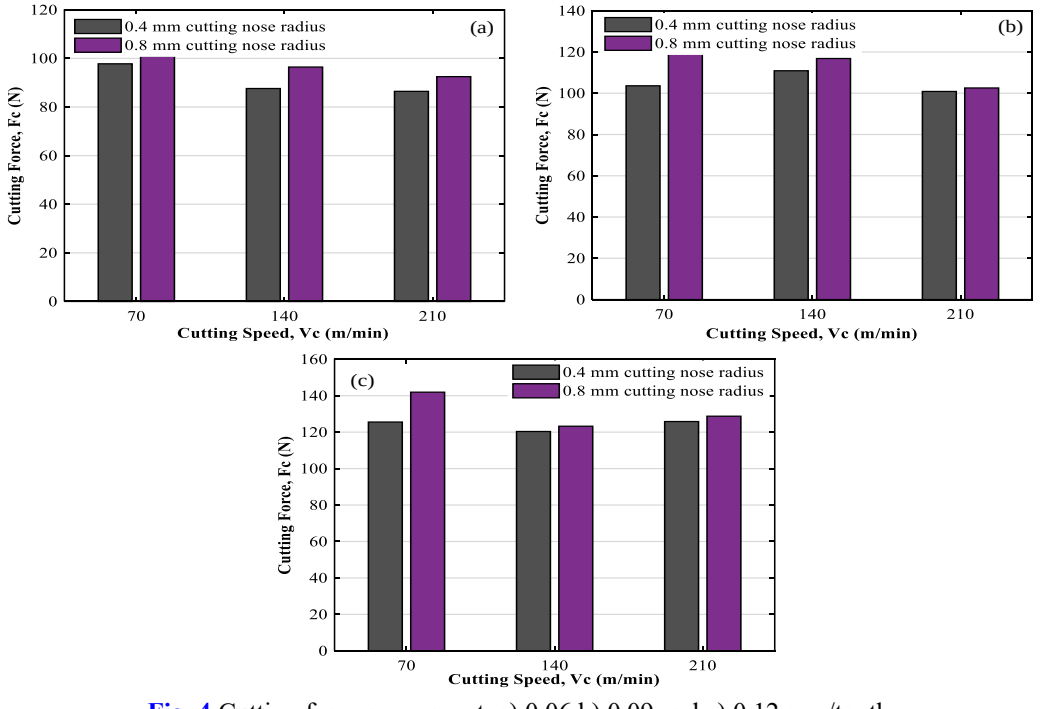

Fig. 4 Cutting force assessment, a) 0.06 b) 0.09 and c) 0.12 mm/tooth.

Table 4. Result of variance for the output parameters.

Factors	Degree of freedom (DoF)	Sum of squares (SS)	Mean square (MS)	F ratio	P ratio	Contribution rate (%)
Fc						
Cutting nose radius	1	28.96	28.96	0.74	0.4063	0.72
Cutting speed	2	87.17	43.59	1.12	0.3596	2.16
Feed rate	2	3451.31	1725.66	44.15	0.0000	85.50
Error	12	469.02	39.08			11.62
Total	17	4036.46				100
Ra						
Cutting nose radius	1	0.1764	0.1764	296.89	0.0000	73.91
Cutting speed	2	0.0398	0.0199	33.53	0.0000	16.69
Feed rate	2	0.0153	0.0076	12.88	0.0001	6.41
Error	12	0.0071	0.0005			2.99
Total	17	0.2386				100
T						
Cutting nose radius	1	16989.4	16989.4	269.13	0.0000	48.70
Cutting speed	2	13960.4	6980.2	110.57	0.0000	40.02
Feed rate	2	3177.2	1588.6	25.16	0.0001	9.11
Error	12	757.5	63.1			2.17
Total	17	34884.5				100
Vb						
Cutting nose radius	1	0.000001	0.000001	0.01	0.925	0.02
Cutting speed	2	0.001703	0.000852	14.69	0.001	57.27
Feed rate	2	0.000574	0.000287	4.95	0.027	19.31
Error	12	0.000696	0.000058			23.40
Total	17	0.002974				100

rate is about 28 and 45% by the 100% increase of feed rate, respectively. This situation may be explained by the tool-chip contact area and the volume of material removed increases and resulting in the Fc increases and is compatible with the literature knowledge. Moreover, Leksycki *et al*. reported that the feed rate was effective over the cutting forces when finish turning of 17-4 PH steel.[33] On the other hand, cutting force decreased along with the increase in cutting speed. In milling with 0.4 mm cutting nose radius, the cutting force values at 70, 140, and 210 m/min cutting speed were measured at 97.42, 87.62, and 86.45 N, respectively. It decreased by approximately 10.49 and 11.58% at other cutting speeds, respectively compared to the 70 m/min cutting speed. Under the same cutting condition, the cutting force values were measured at 100.86, 96.45, and 92.50 N in milling with a 0.8 mm cutting nose radius, respectively. A similar trend was observed in milling with a 0.8 mm cutting nose radius. Liu *et al*. reported that cutting forces decreased with the increasing cutting speed in turning 17-4 PH steel with different textured cutting tools.[34] In another study, Sivaiah and Chakradhar, when turning 17-4 PH steel, obtained a similar result, and the authors argued that this decreasing trend was due to an increase in cutting temperature and a reduction in chip thickness.[35]

4.4 Surface roughness

The average surface roughness (Ra) statement is generally used to express the surface quality of the workpiece in machining operations. Fig. 5 presents the effects of cutting parameters and nose radius on the average surface roughness (Ra). Three measurements were made on each machined surface and the surface roughness values are calculated as the average of three measurements. The Ra values ranged from 0.141 to 0.511 µm. As can be seen from Fig. 5, surface roughness was significantly affected by nose radius, cutting speed and feed rate, respectively. Considering the average of all roughness values measured when the workpiece is machined with 0.4 and 0.8 the cutting nose radius, an average of 47.48% improvement in surface quality was observed in test measurements when 17-4 PH stainless steel is machined with 0.8 the cutting nose radius. This situation can be associated with the amplitude of the surface profile is decreased due to the extended contact zone in the operation.[36] Gürgen *et al*. have also been reported that when machining the

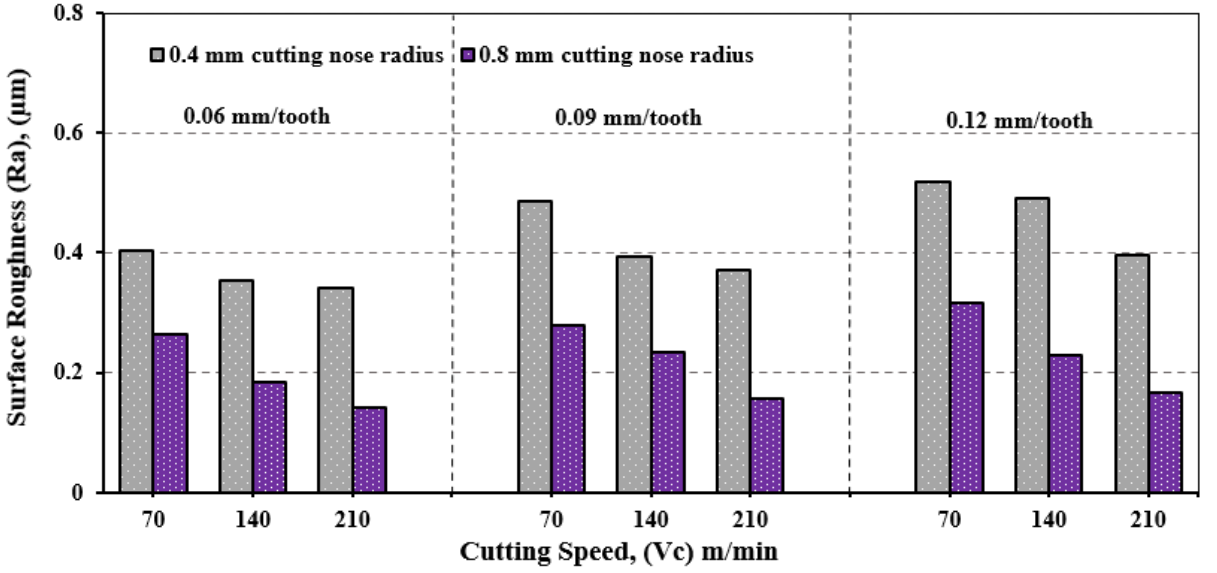

Fig. 5 Surface roughness assessment.

workpiece with small nose radius, it may cause an increase in the pitch of the surface profile.[37] It has been also observed that the surface roughness values obtained at 140 m/min cutting speed are approximately 20-25% lower than the surface roughness values obtained at 70 m/min cutting speed, and the surface roughness values are reduced by approximately 40% with a further increase in cutting speed to 210 m/min. This situation can be explained by the decrease in the tool-chip contact area and the decrease in the shear strength of the material with the increase in temperature depending on the increase in cutting speed,[7,38,39] On the other hand, it is seen that the surface roughness (Ra) values increase with increasing feed rate in all cutting parameters for both tools. Depending on the increase in the feed rate, the surface roughness values increase as a result of more chip volume removed per unit time.[40,41] Özbek *et al*. found similar result and it was concluded that the feed rate can be selected at medium levels.[42] As is displayed in Table 4, the most effective parameter on the surface quality of the workpiece is the tool nose radius with 73.91% contribution rate. Compared to the tool nose radius, the cutting speed and feed rate have less effect on the formation of surface roughness. The cutting nose radius is effective in forming surface roughness was also reported by other researchers.[36,43] Fig. 6 shows the surface profile images of the machined surfaces for the lowest surface roughness values obtained at 210 m/min cutting speed and 0.06 mm/rev feed rate. When Fig. 6 is examined, compared to the surface obtained at 0.8 mm cutting nose radius, it is seen that the depth and width of the craters formed on the surface obtained at 0.4 mm cutting nose radius are larger and the surface roughness value increases accordingly.

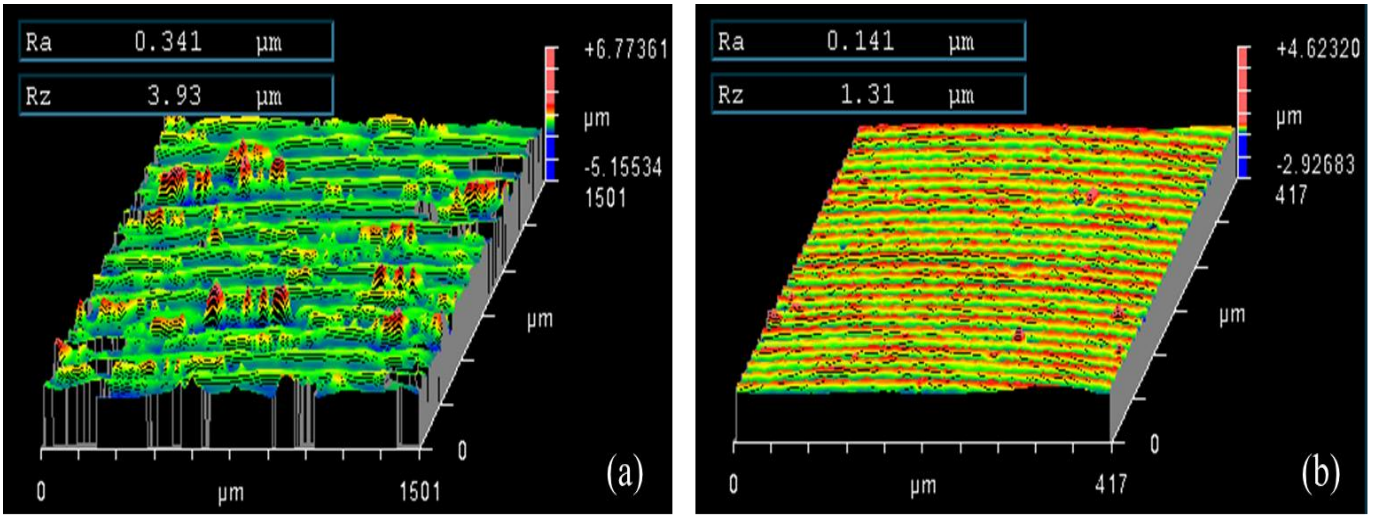

Fig. 6 Three-dimensional surface profile images of the machined surfaces at optimum process parameters with a) 0.4 mm and b) 0.8 mm cutting nose radius.

4.5 Cutting temperature

The effect of cutting nose radius and cutting parameters on the cutting temperature is shown in Fig. 7. In both cutting tools, the cutting temperature values exhibited an increasing tendency with increasing cutting speed. Similarly, the increase in the cutting temperature was significantly impacted by an increase in feed rate. The cutting temperature values of 0.09 and 0.12 mm/tooth were increased by 108.67 and 165.74%, respectively compared to 0.06 mm/tooth feed (at 70 m/min cutting speed). Under the same cutting condition, the cutting temperature values of 140 and 210 m/min were increased by 108.67 and 165.74%, respectively compared to 70 m/min cutting speed (at 0.06 mm/tooth feed rate). Sivaiah and Chakradhar reported that the cutting temperature increased by 63-72% by increasing the cutting speed from 25 to 132 m/min in turning of 17-4 PH steel under a dry machining environment.[44] This result may be associated that the increase in strain rate and deformation, which causes the acceleration of tool wear formation with the increase in cutting speed and feed rate as reported by other researchers.[45,42]

The cutting temperature values given in Fig. 7 show that the lowest cutting temperature was obtained at 70 m/min cutting speed, 0.06 mm/rev feed rate, and 0.4 mm cutting nose radius. On the other hand, the highest cutting temperature values was obtained at 210 m/min cutting speed, 0.12 mm/tooth feed rate, and 0.8 mm cutting nose radius. When the average of all temperature results saved in both cutting tools is computed, the cutting temperature measured values when milling 17-4 PH stainless steel with 0.4 mm cutting nose radius is lower by 28.89% than measured values in 0.8 mm cutting nose radius.

4.6 Tool wear

The changes in the flank wear which was obtained as the result of the experimental study are seen in Fig. 8. It is obvious from the surface charts that the tool wear values increase in both tools when the cutting speed is increased. The lowest tool wear was obtained at the lowest cutting speed (70 m/min) and the tool wear increased by increasing the cutting speed. The tool wear values for 0.4- and 0.8-mm cutting nose radius have about a 43 and 38% increase with a 50% increase of the cutting speed while this increased rate is about 25 and 20% by the 100% increase of the cutting speed, respectively. Similarly, an increase in feed rate had a significant effect on increasing tool wear. The tool wear values for 0.4- and 0.8-mm cutting nose radius have average 16% increase with increasing feed rate as 50%, while average 10% increase by increasing feed rate as 100%, respectively. Increasing the cutting speed and feed rate raises the temperatures in the cutting zone, resulting in increased thermal and mechanical loads, which accelerates the deformation of the cutting tool.[39] When the average of all tool wear measurements obtained for the two cutting tools was calculated, it was seen that the wear values measured in the experiments using cutting tools with a 0.4 mm cutting nose radius were 1.18% lower than the wear values measured in the experiments using cutting tools with a 0.8 mm cutting nose radius. This is attributed to the fact that as the cutting temperature increases with increasing cutting tool tip radius, the cutting tool wears faster and in smaller chip volumes. Moreover, as the cutting tool tip radius increases, friction

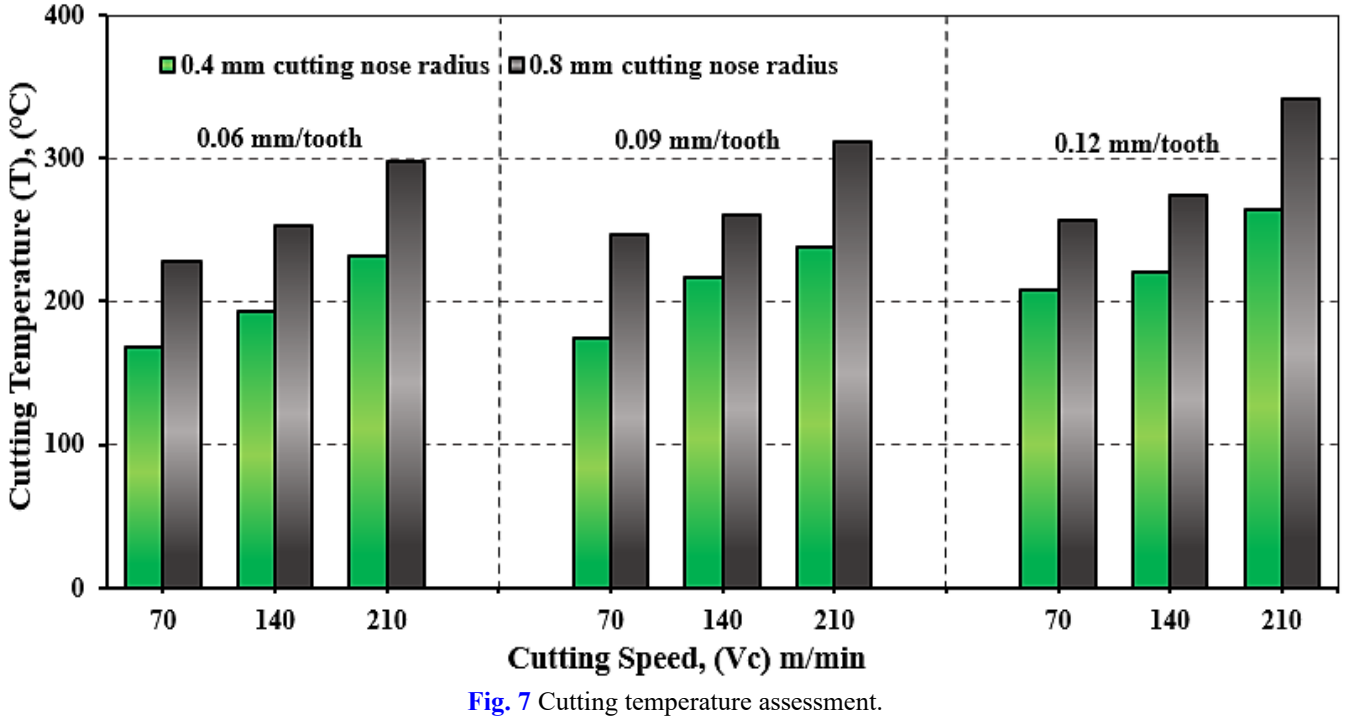

Fig. 7 Cutting temperature assessment.

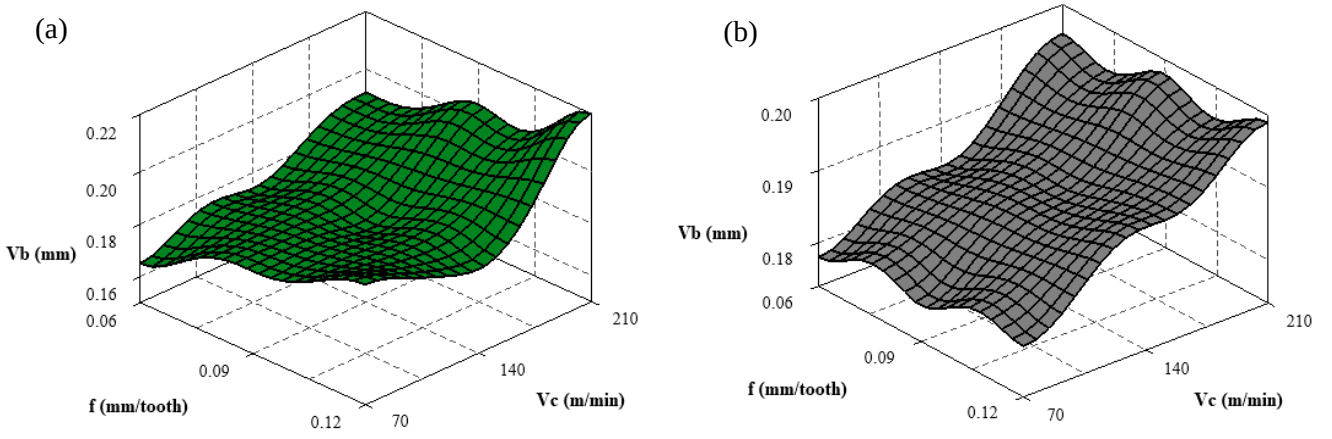

Fig. 8 Tool wear assessment, a) 0.4 mm and b) 0.8 mm cutting nose radius.

Table 5. Result of variance for the output parameters.

	Experimental results				Normalize values				Gray relational coefficient				GRG	S/N ration	Order
	Fc	T	Ra	Vb	Fc	T	Ra	Vb	Fc	T	Ra	Vb			
1	97.42	168	0.403	0.165	0.811	1.000	0.307	1.000	0.726	1.000	0.419	1.000	0.786	-2.091	1
2	103.62	174	0.487	0.181	0.583	0.965	0.083	0.709	0.545	0.935	0.353	0.632	0.616	-4.208	7
3	125.54	208	0.518	0.196	0.000	0.769	0.000	0.456	0.333	0.684	0.333	0.479	0.457	-6.801	17
4	92.5	193	0.354	0.174	1.000	0.855	0.437	0.842	1.000	0.776	0.471	0.760	0.752	-2.475	2
5	110.91	217	0.394	0.179	0.461	0.717	0.331	0.754	0.481	0.638	0.428	0.671	0.554	-5.129	11
6	120.36	221.6	0.49	0.182	0.343	0.690	0.075	0.702	0.432	0.617	0.351	0.626	0.507	-5.899	16
7	98.6	231.7	0.341	0.191	0.963	0.632	0.472	0.544	0.930	0.576	0.486	0.523	0.629	-4.026	6
8	100.88	238	0.372	0.206	0.722	0.595	0.389	0.281	0.643	0.553	0.450	0.410	0.514	-5.780	15
9	125.82	264	0.397	0.222	0.242	0.445	0.323	0.000	0.398	0.474	0.425	0.333	0.407	-7.808	18
10	97.78	228	0.265	0.178	0.818	0.653	0.675	0.772	0.733	0.590	0.606	0.687	0.654	-3.688	4
11	110.19	247	0.278	0.179	0.704	0.543	0.640	0.754	0.628	0.523	0.581	0.671	0.601	-4.422	9
12	141.93	256.6	0.317	0.181	0.301	0.488	0.536	0.719	0.417	0.494	0.519	0.640	0.518	-5.713	14
13	87.52	253	0.184	0.184	0.908	0.509	0.891	0.667	0.845	0.504	0.821	0.600	0.693	-3.185	3
14	116.85	259.1	0.234	0.187	0.570	0.473	0.757	0.605	0.538	0.487	0.673	0.559	0.564	-4.974	10
15	123.25	274.3	0.228	0.191	0.396	0.386	0.773	0.544	0.453	0.449	0.688	0.523	0.528	-5.547	12
16	89.56	298.3	0.141	0.196	0.796	0.247	1.000	0.456	0.711	0.399	1.000	0.479	0.647	-3.781	5
17	102.65	311	0.157	0.198	0.754	0.173	0.963	0.421	0.671	0.377	0.931	0.463	0.610	-4.293	8
18	128.75	341	0.168	0.199	0.296	0.000	0.933	0.404	0.415	0.333	0.882	0.456	0.522	-5.646	13

increases as a result of the increase in the tool-chip contact area. Since the increased friction is directly proportional to the cutting force, the force on the cutting tool also increases and as a result, the wear of the cutting tool accelerates.

4.7 Multi response optimization

Gray relational analysis, a multi-response optimization technique, was used to determine the optimum processing conditions for all output parameters (cutting force, surface roughness, cutting temperature, and tool wear), which is one of the objectives of the study. This method is a widely used method for optimization of multiple response problems in the metal cutting industry.[46] The main point of this method is to simultaneously determine the optimum combination of process parameters according to multiple performance characteristics. In this context, experimental data were first normalized first to be in the range of zero to one. The gray relational coefficient was calculated for the normalized data. Then, the gray relational grade (GRG) was obtained by averaging the GRA coefficient. Thus, the multi-response optimization problem was transformed into a single objective function by obtaining gray relational degrees for each performance output.[47] The higher the gray relationship degree value for process parameter combination, the closer it is to the optimal result. The gray relationship analysis process results for output parameters are given in Table 5. From Table 5, the optimal combination of process parameters for output parameters is found to be: $A_1B_1C_1$. This combination also is optimal according to the S/N response results for the GRG is given in Table 6. Table 7 summarizes the optimum process parameters obtained using the Taguchi approach and grey relational analysis in the milling of 17-4 PH stainless steel.

Table 6. Answer table for GRG.

Code	Grey Relational Grade				
	Level 1	Level 2	Level 3	Delta	Rank
A	-4.914	-4.584	-	0.330	3
B	-4.488	-4.535	-5.233	0.735	2
C	-3.208	-4.802	-6.236	3.028	1

Average of total gray relationship grade=0.586.

Table 7. Optimum levels of process conditions for output parameters.

Output parameter	Analysis method	Optimal process factors
Ra	Taguchi	A2B3C1
Fc	Taguchi	A1B3C1
T	Taguchi	A1B1C1
Vb	Taguchi	A1B1C1
Fc, Ra, T and Vb	Grey relational analysis	A2B1C1

5. Conclusions

This paper is concerned with determining the optimum settings of process parameters for multi-response optimization during the milling of 17-4 PH stainless steel using the Taguchi grey relational approach. Cutting force, surface roughness, cutting temperature and tool wear have been considered as multiple response outputs. The major conclusions can be summarized as follows:

- The optimal combination of process parameters for Ra is found to be: $A_2B_3C_1$ (i.e., cutting nose radius= 0.8 mm, cutting speed=210 m/min and feed rate=0.06 mm/tooth).
- The optimal combination of process parameters for Fc is found to be: $A_1B_3C_1$ (i.e., cutting nose radius= 0.4 mm, cutting speed=210 m/min and feed rate=0.06 mm/tooth).
- The optimal combination of process parameters for T and Vb are found to be: $A_1B_1C_1$ (i.e., cutting nose radius= 0.8 mm, cutting speed=70 m/min and feed rate=0.06 mm/tooth).
- According to the grey correlation analysis results, the optimal combination of process parameters for multiple output parameters (Fc, Ra, T and Vb) is determined as $A_2B_1C_1$ (i.e., cutting nose radius= 0.8 mm, cutting speed=70 m/min and feed rate=0.06 mm/tooth).
- According to ANOVA results, cutting nose radius is the most influential factor in Ra and T. Feed rate and cutting speed is also the most influential factor in Fc and Vb, respectively.
- In general, all output parameters increased with increasing feed rate.
- The lowest surface roughness values were measured when 17-4 PH stainless steel is machined with 0.8 mm cutting nose radius. According to all test conditions, the surface roughness values in experiments using 0.8 mm cutting nose radius was found less by average 47.48% than those in experiments using 0.4 mm cutting nose radius.
- This martensitic stainless steel should be machined at medium cutting speed and feed rate to obtain high surface quality. The cutting nose radius has also a considerable effect on the surface roughness.

Conflict of Interest

There is no conflict of interest.

Supporting Information

Not applicable.

References

[1] M. E. Korkmaz, Verification of Johnson-Cook parameters of ferritic stainless steel by drilling process: experimental and finite element simulations, *Journal of Materials Research and Technology*, 2020, **9**, 6322-6330, doi: 10.1016/j.jmrt.2020.03.045.

[2] M. C. Karthik Rao, R. L. Malghan, A. K. Shettigar, S. S. Rao, M. A. Herbert, Application of back propagation algorithms in neural network based identification responses of AISI 316 face milling cryogenic machining technique, *Australian Journal of Mechanical Engineering*, 2022, **20**, 698-705, doi: 10.1080/14484846.2020.1740022.
[3] J. D. Bressan, D. P. Daros, A. Sokolowski, R. A. Mesquita, C. A. Barbosa, Influence of hardness on the wear resistance of 17-4 PH stainless steel evaluated by the pin-on-disc testing, *Journal of Materials Processing Technology*, 2008, **205**, 353-359, doi: 10.1016/j.jmatprotec.2007.11.251.
[4] P. Kochmański, J. Nowacki, Activated gas nitriding of 17-4 PH stainless steel, *Surface and Coatings Technology*, 2006, **200**, 6558-6562, doi: 10.1016/j.surfcoat.2005.11.034.
[5] P. Kochmanski, J. Nowacki, Influence of initial heat treatment of 17-4 PH stainless steel on gas nitriding kinetics, *Surface and Coatings Technology*, 2008, **202**, 4834-4838, doi: 10.1016/j.surfcoat.2008.04.058.
[6] J. Yao, L. Wang, Q. Zhang, F. Kong, C. Lou, Z. Chen, Surface laser alloying of 17-4PH stainless steel steam turbine blades, *Optics & Laser Technology*, 2008, **40**, 838-843, doi: 10.1016/j.optlastec.2007.11.008.
[7] I. Ciftci, Machining of austenitic stainless steels using CVD multi-layer coated cemented carbide tools, *Tribology International*, 2006, **39**, 565-569, doi: 10.1016/j.triboint.2005.05.005.
[8] S. Huang, T. Lv, X. Xu, Y. Ma, M. Wang, Experimental evaluation on the effect of electrostatic minimum quantity lubrication (EMQL) in end milling of stainless steels, *Machining Science and Technology*, 2018, **22**, 271-286, doi: 10.1080/10910344.2017.1337135.
[9] A. Mohanty, S. Gangopadhyay, A. Thakur, On applicability of multilayer coated tool in dry machining of aerospace grade stainless steel, *Materials and Manufacturing Processes*, 2016, **31**, 869-879, doi: 10.1080/10426914.2015.1070413.
[10] N. Khanna, P. Shah, Chetan, Comparative analysis of dry, flood, MQL and cryogenic CO_2 techniques during the machining of 15-5-PH SS alloy, *Tribology International*, 2020, **146**, 106196, doi: 10.1016/j.triboint.2020.106196.
[11] M. Kumar Gupta, M. Boy, M. Erdi Korkmaz, N. Yaşar, M. Günay, G. M. Krolczyk, Measurement and analysis of machining induced tribological characteristics in dual jet minimum quantity lubrication assisted turning of duplex stainless steel, *Measurement*, 2022, **187**, 110353, doi: 10.1016/j.measurement.2021.110353.
[12] P. Sivaiah, D. Chakradhar, Effect of cryogenic coolant on turning performance characteristics during machining of 17-4 PH stainless steel: a comparison with MQL, wet, dry machining, *CIRP Journal of Manufacturing Science and Technology*, 2018, **21**, 86-96, doi: 10.1016/j.cirpj.2018.02.004.
[13] P. Sivaiah, D. Chakradhar, Performance improvement of cryogenic turning process during machining of 17-4 PH stainless steel using multi objective optimization techniques, *Measurement*, 2019, **136**, 326-336, doi: 10.1016/j.measurement.2018.12.094.
[14] N. Khanna, P. Shah, M. Sarikaya, F. Pusavec, Energy consumption and ecological analysis of sustainable and conventional cutting fluid strategies in machining 15-5 PHSS, *Sustainable Materials and Technologies*, 2022, **32**, e00416, doi: 10.1016/j.susmat.2022.e00416.
[15] E. Nas, N. Altan Özbek, Optimization of the machining parameters in turning of hardened hot work tool steel using cryogenically treated tools, *Surface Review and Letters,* 2020, **27**, 1950177, doi: 10.1142/S0218625X19501774.
[16] K. Gurpur Vignesh, B. P. Achar, A. M. Hebbale, Correlation analysis of Machining parameters against cutting forces during Machining of 17-4 PHSS using cryogenic treated and untreated WC insert, *Materials Today: Proceedings*, 2022, **52**, 1639-1643, doi: 10.1016/j.matpr.2021.11.279.
[17] O. Öndin, T. Kıvak, M. Sarıkaya, Ç. V. Yıldırım, Investigation of the influence of MWCNTs mixed nanofluid on the machinability characteristics of PH 13-8 Mo stainless steel, *Tribology International*, 2020, **148**, 106323, doi: 10.1016/j.triboint.2020.106323.
[18] P. Sivaiah, M. Singh, V. Chengal Reddy, P. Meghashyam, Processing of 17-4 PH steel in turning operation with hybrid textured tools, *Materials and Manufacturing Processes*, 2022, **37**, 241-250, doi: 10.1080/10426914.2021.2001503.
[19] P. Sivaiah, D. Chakradhar, The effectiveness of a novel cryogenic cooling approach on turning performance characteristics during machining of 17-4 PH stainless steel material, *Silicon*, 2019, **11**, 25-38, doi: 10.1007/s12633-018-9875-3.
[20] P. Sivaiah, B. Uma, Multiobjective optimization of sustainable turning process using TOPSIS method, *Emerging Materials Research*, 2019, **8**, 686-695, doi: 10.1680/jemmr.17.00029.
[21] E. Nas, Analysis of the electrical discharge machining (EDM) performance on Ramor 550 armor steel, *Materials Testing,* 2020, **62**, 481-491, doi:10.3139/120.111510.
[22] P. Sivaiah, D. Chakradhar, Multi performance characteristics optimization in cryogenic turning of 17-4 PH stainless steel using Taguchi coupled grey relational analysis, *Advances in Materials and Processing Technologies*, 2018, **4**, 431-447, doi: 10.1080/2374068x.2018.1452132.
[23] G. Liu, B. Zou, C. Huang, X. Wang, J. Wang, Z. Liu, Tool damage and its effect on the machined surface roughness in high-speed face milling the 17-4PH stainless steel, *The International Journal of Advanced Manufacturing Technology*, 2016, **83**, 257-264, doi: 10.1007/s00170-015-7564-6.
[24] A. Bagherzadeh, E. Kuram, E. Budak, Experimental evaluation of eco-friendly hybrid cooling methods in slot milling of titanium alloy, *Journal of Cleaner Production*, 2021, **289**, 125817, doi: 10.1016/j.jclepro.2021.125817.
[25] E. Nas, O. Özbek, F. Bayraktar, F. Kara, Experimental and statistical investigation of machinability of AISI D2 steel using electroerosion machining method in different machining parameters, *Advances in Materials Science and Engineering*, 2021, **2021**, 1-17, doi: 10.1155/2021/1241797.
[26] R. Lmalghan, K. Rao M C, S. ArunKumar, S. S. Rao, M. A. Herbert, Machining parameters optimization of AA6061 using

response surface methodology and particle swarm optimization, *International Journal of Precision Engineering and Manufacturing*, 2018, **19**, 695-704, doi: 10.1007/s12541-018-0083-2.
[27] N. Yaşar, Thrust force modelling and surface roughness optimization in drilling of AA-7075: FEM and GRA, *Journal of Mechanical Science and Technology*, 2019, **33**, 4771-4781, doi: 10.1007/s12206-019-0918-5.
[28] M. Günay, E. Yücel, Application of Taguchi method for determining optimum surface roughness in turning of high-alloy white cast iron, *Measurement*, 2013, **46**, 913-919, doi: 10.1016/j.measurement.2012.10.013.
[29] E. Nas, F. Kara, Optimization of EDM Machinability of Hastelloy C22 Super Alloys, *Machines,* 2022, **10**, 1131, doi:10.3390/machines10121131.
[30] I. V. Manoj, H. Soni, S. Narendranath, P. M. Mashinini, F. Kara, Examination of machining parameters and prediction of cutting velocity and surface roughness using RSM and ANN using WEDM of altemp HX, *Advances in Materials Science and Engineering*, 2022, **2022**, 1-9, doi: 10.1155/2022/5192981.
[31] A. K. Parida, K. Maity, Effect of nose radius on forces, and process parameters in hot machining of Inconel 718 using finite element analysis, *Engineering Science and Technology, an International Journal*, 2017, **20**, 687-693, doi: 10.1016/j.jestch.2016.10.006.
[32] F. Kara, F. Bayraktar, F. Savaş, O. Özbek, Experimental and statistical investigation of the effect of coating type on surface roughness, cutting temperature, vibration and noise in turning of mold steel, *Journal of Materials and Manufacturing*, 2023, **2**, 31-43, doi:10.5281/zenodo.8020553.
[33] K. Leksycki, E. Feldshtein, J. Lisowicz, R. Chudy, R. Mrugalski, Cutting forces and chip shaping when finish turning of 17-4 PH stainless steel under dry, wet, and MQL machining conditions, *Metals*, 2020, **10**, 1187, doi: 10.3390/met10091187.
[34] G. Liu, C. Huang, R. Su, T. Özel, Y. Liu, L. Xu, 3D FEM simulation of the turning process of stainless steel 17-4PH with differently texturized cutting tools, *International Journal of Mechanical Sciences*, 2019, **155**, 417-429, doi: 10.1016/j.ijmecsci.2019.03.016.
[35] P. Sivaiah, D. Chakradhar, Comparative evaluations of machining performance during turning of 17-4 PH stainless steel under cryogenic and wet machining conditions, *Machining Science and Technology*, 2018, **22**, 147-162, doi: 10.1080/10910344.2017.1337129.
[36] A. C. Basheer, U. A. Dabade, S. S. Joshi, V. V. Bhanuprasad, V. M. Gadre, Modeling of surface roughness in precision machining of metal matrix composites using ANN, *Journal of Materials Processing Technology*, 2008, **197**, 439-444, doi: 10.1016/j.jmatprotec.2007.04.121.
[37] M. Akgün, H. Demir, Optimization of cutting parameters affecting surface roughness in turning of Inconel 625 superalloy by cryogenically treated tungsten carbide inserts, *SN Applied Sciences*, 2021, **3**, 1-12, doi: 10.1007/s42452-021-04303-2.
[38] E. M. Trent, Metal cutting. London: Butterworths Press, ed. Third Edition, 1989.
[39] B. Özlü, H. Demir, M. Türkmen, S. Gündüz, Examining the machinability of 38MnVS6 microalloyed steel, cooled in different mediums after hot forging with the coated carbide and ceramic tool, *Proceedings of the Institution of Mechanical Engineers, Part C: Journal of Mechanical Engineering Science*, 2021, **235**, 6228-6239, doi: 10.1177/0954406220984498.
[40] A. I. Fernández-Abia, J. Barreiro, L. N. L. de Lacalle, S. Martínez, Effect of very high cutting speeds on shearing, cutting forces and roughness in dry turning of austenitic stainless steels, *The International Journal of Advanced Manufacturing Technology*, 2011, **57**, 61-71, doi: 10.1007/s00170-011-3267-9.
[41] A. Lamikiz, L. N. López de Lacalle, J. A. Sánchez, M. A. Salgado, Cutting force estimation in sculptured surface milling, *International Journal of Machine Tools and Manufacture*, 2004, **44**, 1511-1526, doi: 10.1016/j.ijmachtools.2004.05.004.
[42] N. Altan Özbek, O. Özbek, F. Kara, Statistical analysis of the effect of the cutting tool coating type on sustainable machining parameters, *Journal of Materials Engineering and Performance*, 2021, **30**, 7783-7795, doi: 10.1007/s11665-021-06066-8.
[43] M. Akgün, H. Demir, Estimation of surface roughness and flank wear in milling of inconel 625 superalloy, *Surface Review and Letters*, 2021, **28**, 2150011, doi: 10.1142/s0218625x21500116.
[44] P. Sivaiah, D. Chakradhar, Machinability studies on 17-4 PH stainless steel under cryogenic cooling environment, *Materials and Manufacturing Processes*, 2017, **32**, 1775-1788, doi: 10.1080/10426914.2017.1339317.
[45] A. Thakur, S. Gangopadhyay, K. P. Maity, S. K. Sahoo, Evaluation on effectiveness of CVD and PVD coated tools during dry machining of incoloy 825, *Tribology Transactions*, 2016, **59**, 1048-1058, doi: 10.1080/10402004.2015.1131350.
[46] M. Akgün, Performance analysis of electrode materials in electro discharge machining of monel K-500, *Surface Topography: Metrology and Properties*, 2022, **10**, 035026, doi: 10.1088/2051-672x/ac8d19.
[47] B. Özlü, Experimental and statistical investigation of the effects of cutting parameters on kerf quality and surface roughness in laser cutting of Al 5083 alloy, *Surface Review and Letters*, 2021, **28**, 2150093, doi: 10.1142/s0218625x21500931.

